



Molecular Crystals and Liquid Crystals

Publication details, including instructions for authors and subscription information:

<http://www.tandfonline.com/loi/gmcl20>

Effect of Substrate Temperature on Preferred Orientation and Ga Composition Profile of Co-Evaporated Cu(In,Ga)Se₂

Soon-Rok Park^a, Ju-Young Baek^a, Tae-Young Yun^a, Hye-Jin Han^a,
Kyoung-Bo Kim^b & Chan-Wook Jeon^a

^a Department of Chemical Engineering, Yeungnam University,
Gyeongsan, Gyeongbuk, 712-749, Korea

^b Surface Technology Research Group, POSCO Technical Research
Laboratories, Incheon, Korea

Published online: 08 Jan 2014.

To cite this article: Soon-Rok Park, Ju-Young Baek, Tae-Young Yun, Hye-Jin Han, Kyoung-Bo Kim & Chan-Wook Jeon (2013) Effect of Substrate Temperature on Preferred Orientation and Ga Composition Profile of Co-Evaporated Cu(In,Ga)Se₂, Molecular Crystals and Liquid Crystals, 585:1, 114-120, DOI: [10.1080/15421406.2013.850941](https://doi.org/10.1080/15421406.2013.850941)

To link to this article: <http://dx.doi.org/10.1080/15421406.2013.850941>

PLEASE SCROLL DOWN FOR ARTICLE

Taylor & Francis makes every effort to ensure the accuracy of all the information (the "Content") contained in the publications on our platform. However, Taylor & Francis, our agents, and our licensors make no representations or warranties whatsoever as to the accuracy, completeness, or suitability for any purpose of the Content. Any opinions and views expressed in this publication are the opinions and views of the authors, and are not the views of or endorsed by Taylor & Francis. The accuracy of the Content should not be relied upon and should be independently verified with primary sources of information. Taylor and Francis shall not be liable for any losses, actions, claims, proceedings, demands, costs, expenses, damages, and other liabilities whatsoever or howsoever caused arising directly or indirectly in connection with, in relation to or arising out of the use of the Content.

This article may be used for research, teaching, and private study purposes. Any substantial or systematic reproduction, redistribution, reselling, loan, sub-licensing, systematic supply, or distribution in any form to anyone is expressly forbidden. Terms &

Effect of Substrate Temperature on Preferred Orientation and Ga Composition Profile of Co-Evaporated Cu(In,Ga)Se₂

SOON-ROK PARK,¹ JU-YOUNG BAEK,¹ TAE-YOUNG YUN,¹
HYE-JIN HAN,¹ KYOUNG-BO KIM,²
AND CHAN-WOOK JEON^{1,*}

¹Department of Chemical Engineering, Yeungnam University, Gyeongsan,
Gyeongbuk 712-749, Korea

²Surface Technology Research Group, POSCO Technical Research Laboratories,
Incheon, Korea

Cu(In,Ga)Se₂ (CIGS) films were deposited by the three-stage co-evaporation process and the effect of the second stage substrate temperature on device performance were evaluated. With increasing the substrate temperature, the preferred orientation of CIGS was found to be changed from (112) to (220), however, the Ga double grading became weaker and nearly flat for the (220) textured CIGS grown at 570°C. Despite of (220) preferred orientation, the conversion efficiency decreased mainly due to the poor fill factor and open circuit voltage. It is suggested that increasing the growth temperature in order to get (220) preferred CIGS may destroy the advantage of double-graded Ga profile.

Keywords CIGS; Cu(In, Ga)Se₂; co-evaporation; three-stage; Ga profile; preferred orientation

Introduction

Cu(In,Ga)Se₂ (CIGS) compound which has high optical absorption coefficient as direct transition type semiconductor, is very profitable in thin film solar cell manufacture. With several advantages, including high thermal stability and moisture tolerance, CIGS-based solar cells have achieved the highest energy conversion efficiency among thin-film photovoltaic technology [1]. World record efficiency for Cu(In,Ga)Se₂ thin-film solar cells reached beyond 20% by three-stage process [2]. The advantage of the process is that the Ga/(In+Ga) ratio can be controlled and increasing Ga concentration towards the back contact improves open-circuit voltage (Voc) and fill factor (FF) due to passivation of the back contact [3]. At 2nd stage, the substrate temperature is rising from 300~400°C to 500°C ~ 600°C for the high conversion efficiency solar cell devices [4]. According to the CIGS pseudo-binary phase diagram, the compositional margin of α - CIGS, which is suitable for photovoltaic absorber layer, is broader at higher temperature up to 600°C ~ 700°C [5]. The

*Address correspondence to , Prof. Chan-Wook Jeon, School of Chemical Engineering, Yeungnam University, Dae-dong, Gyungsan-si, Gyeongbuk, 712-749, Korea (ROK), Tel: (+82)53-810-3860, Fax: (+82)53-810-4631. E-mail: cwjeon@ynu.ac.kr

crystalline quality is expected to be better for the high temperature grown CIGS and hence the device performance would be better due to lower defect density in the high temperature CIGS. [6]. On the other hand, increasing the growth temperature at the second stage could promote diffusion of element, especially Ga, which should be evaluated for implementing a desirable bandgap profile in the absorber film.

In this study, CIGS absorber layer was grown using the three-stage co-evaporation process. The solar cells made of CIGS grown at different substrate temperatures in the second stage were experimentally compared and the effect of variation of growth temperature will be discussed in terms of conversion efficiency

Experimental

A Mo back contact with a thickness $0.6\ \mu\text{m}$ was deposited on a soda-lime glass substrate by DC magnetron sputtering. The CIGS absorber layer was grown by a three-stage co-evaporation of In, Ga, Cu, and Se. In the first stage, an $(\text{In,Ga})_2\text{Se}_3$ layer was grown by co-evaporation In, Ga, Cu and Se elements on the Mo/Glass substrates at 350°C . In the second stage, the substrate temperature was regulated ranging from 530 to 570°C . The end of the second stage was determined by measuring the substrate temperature drop. In the third stage, In, Ga and Se were evaporated on the CIGS layer in order to obtain Cu-poor CIGS film. The fluxes of In, Ga, Cu and Se were fixed at a rate of 2.7 , 0.9 , 2 and $25\ \text{\AA/s}$. The fluxes were monitored by quartz crystal microbalances.

To fabricate CdS/CIGS solar cells, a $50\ \text{nm}$ thick CdS layer was deposited on CIGS film by chemical bath deposition and $i\text{-ZnO}(80\ \text{nm})/n\text{-ZnO:Al}(500\ \text{nm})$ were deposited by magnetron sputtering on the CdS layer. An Al grid ($750\ \text{nm}$) was deposited by DC magnetron sputtering.

Measurements

The current-voltage characteristics of the solar cells were measured under AM1.5 spectrum with $1000\ \text{Wm}^{-2}$ illuminations at 25°C and the capacitance-voltage, incident photon to current efficiency (IPCE) (PEC-S20, Jasco) and secondary ion mass spectroscopy (SIMS) (IMS 6F, CAMECA) depth profiling were measured for the characteristics of the solar cells. The Solar cell's surface images were obtained by scanning electron microscopy (SEM) and the X-ray diffractions were analyzed.

Results and Discussion

Figure 1 shows the plan views of the CIGS's grown at different 2nd stage temperature. The morphologies are quite similar except that the high temperature grown CIGS shows more pronounced faceted structure, which possibly suggests a better crystalline quality [7]. It is interesting to find higher density of small clusters, which are round shape and embedded in the grain boundaries, with increasing the growth temperature. The effect of these particles on the device performance will be discussed later.

Figure 2 shows the X-ray diffraction patterns of the three CIGS's. The $(220)/(112)$ peak ratio abruptly increased for the CIGS layer grown at 570°C . The other two CIGS's grown at the relatively low temperature seems to maintain (112) texture. From the measured full width at half maximum (FWHM) values of $(112)\text{CIGS}$, $(220)\text{CIGS}$, and $(110)\text{Mo}$ reflections, the x-ray coherence lengths were calculated by applying Scherrer's formula

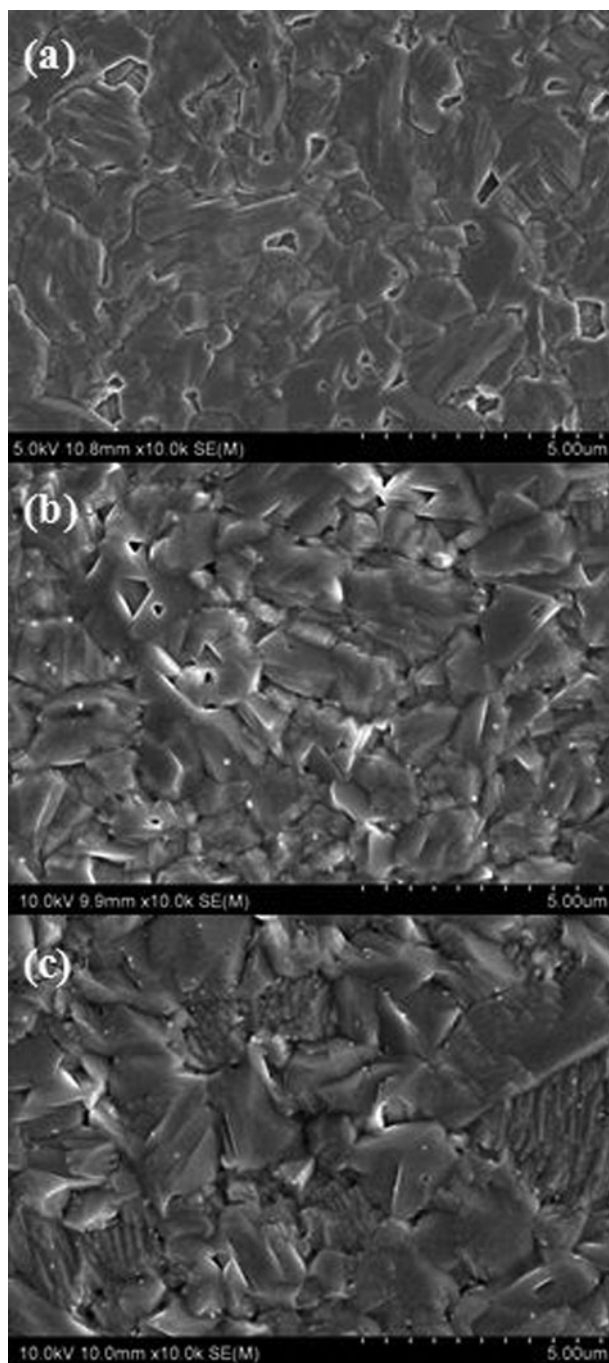


Figure 1. SEM images of the CIGS absorber layers: (a) 530°C, (b) 550°C, and (c) 570°C.

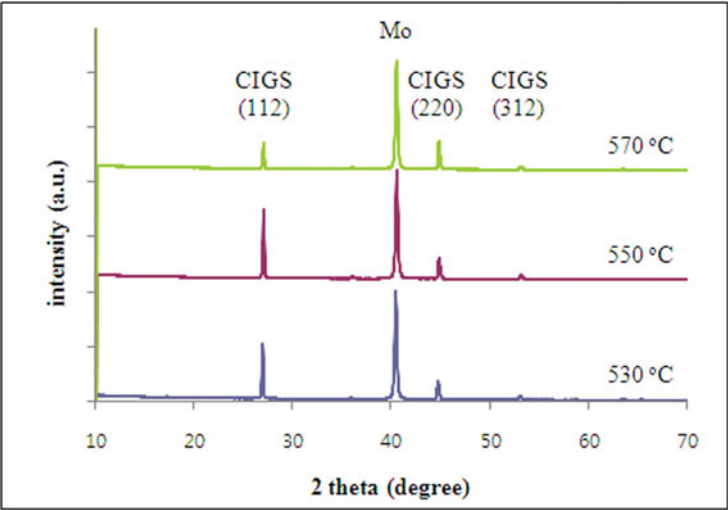


Figure 2. X-ray diffractions patterns of the CIGS absorber layers grown at different temperature.

[8]. and summarized in Table 1. The coherence length doesn't mean the actual grain size of CIGS crystallite because the wavelength of X-ray is by far shorter than the average grain size of co-evaporated CIGS, however, it can be safely assumed to be proportional to the grain size. Referring to the nearly identical values for (110)Mo suggests that the crystalline perfection or simply the grain size increases with increasing the 2nd stage growth temperature. The CIGS absorber film with (220) preferred orientation is known to be beneficial for high efficiency solar cell [9–11]. Contrary to the expectation, however, the CIGS grown at 570°C resulted in the worst photovoltaic performance among the three CIGS's and this will be discussed in the following section.

Figure 3 shows the J-V curve of the solar cells having CIGS's grown at different temperature of 530, 550 and 570°C in the second stage. The solar cell grown at the 530°C showed the best performance, which has a conversion efficiency of 14.85% with short-circuit current density (J_{sc}) = 34.59 mA/cm², V_{oc} = 0.586 V and FF = 73.24% in the total area of 0.49 cm². The performance parameters are summarized in Table 2. The (220/204) oriented films was reported to have lower bandgap energy than the (112) oriented films, [11]. and the higher conversion efficiencies achieved with the (220/204) oriented absorbers were mainly due to increased fill factors and lower sheet resistances, whereas the J_{sc} and V_{oc} were in most cases only moderately higher. However, the devices in this study behave in the complete opposite way to the expectation, that is, all the parameters including V_{oc} , J_{sc} , the reverse saturation current (J_0), and the fill factor were deteriorated with increasing

Table 1. Domain size variation of CIGS films grown at different 2nd stage temperature.

	530°C	550°C	570°C
(112) CIGS (nm)	42.55	42.55	53.20
(220) CIGS (nm)	27.97	37.28	44.74
(110) Mo (nm)	36.43	36.75	36.74

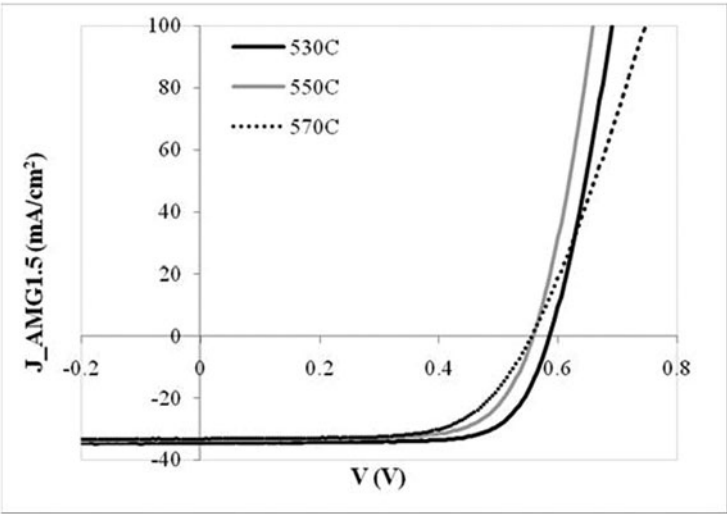


Figure 3. Illuminated J-V curves of the CIGS solar cells.

the 2nd stage temperature despite of outstanding (220) texture. In order to investigate the reason for the loss of V_{oc} and J_{sc} , the external quantum efficiency was measured. It is clearly observed in Figure 4 that the minimum band gap energy, which corresponds to the cut-off value at long wavelength, shifted to higher energy from 1.07 eV to 1.20 eV with increasing substrate temperature. This may be responsible for the modest loss of J_{sc} due to the reduced spectral range but doesn't fit with the loss of V_{oc} at all. The variation of the minimum bandgap energy was found to be well consistent with the actual band profile determined from the Ga depth profile in the secondary ion mass spectroscopy (SIMS) as shown in Figure 5. The average Ga ratios across film thickness were found to be varying from 0.29 for CIGS grown at 530°C to 0.31 for 570°C, which were also confirmed by inductively coupled plasma atomic emission spectroscopy (ICP-AES) analysis, however, such a small variation doesn't account for the device performance variation. In fact, the open circuit voltage for the CIGS with higher Ga was found to be lower in this study. Obviously, the initial double-graded band profile was heavily weakened with increasing the 2nd stage temperature and eventually disappeared at 570°C. It is interesting to note that

Table 2. The photovoltaic parameters of the CIGS solar cells

	530°C	550°C	570°C
J_{sc} (mA/cm ²)	34.59	33.78	33.28
V_{oc} (V)	0.586	0.558	0.556
FF (%)	73.24	69.77	65.56
Efficiency (%)	14.85	13.16	12.13
R_{sh} (ohm cm ²)	9046	3049	3602
R_s (ohm cm ²)	0.51	0.42	1.43
J_o (mA/cm ²)	7.0e – 6	2.4e – 5	3.4e – 4
Ideality factor	1.54	1.59	2.11

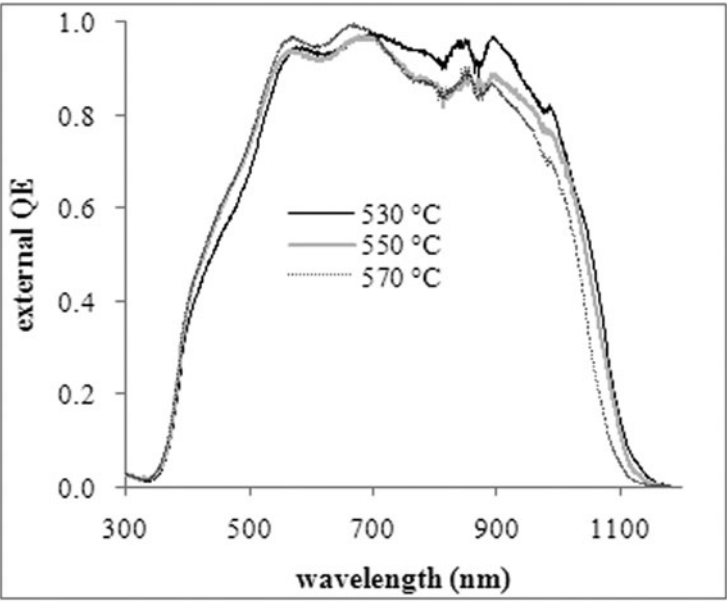


Figure 4. External quantum efficiency of the CIGS solar cells.

surface bandgap energy is nearly identical for the three absorbers. The flattening of the band profile is definitely originated from the enhanced diffusion of Ga at higher growth temperature, however, it cannot reduce the V_{oc} unless the bandgap energy in the space charge region (SCR) decreases [12]. One thing that might be relevant to the loss of V_{oc} and FF, could be found in the surface morphology in Figure 1. The density of the tiny crystallites on the CIGS surface increases with increasing the growth temperature. Assuming they are $Cu_{2-x}Se$, the enhanced surface recombination would decrease V_{oc} and FF [13,14]. In fact, J_o values are substantially higher for the devices made of CIGS's grown at the higher

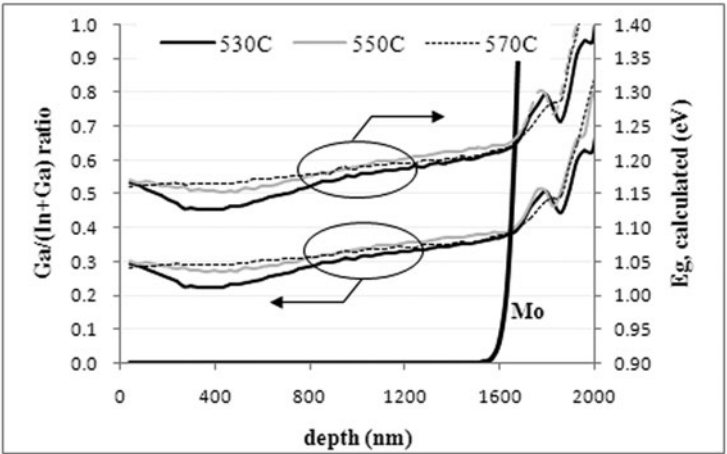


Figure 5. SIMS depth profiles of Ga and the calculated bandgap energy.

temperatures, and especially the device for 570°C was found to have an ideality factor greater than 2, which means the interface recombination limits the device performance. It is not clear yet why the Cu_{2-x}Se phases are formed more heavily at higher growth temperature and even whether they are Cu_{2-x}Se phases or not. Nevertheless, it is suggested that the (220) preferred orientation doesn't guarantee the high efficiency device and an excessive growth temperature may destroy the double-graded bandgap profile.

Conclusions

The CIGS thin film absorbers were deposited using the 3-stage co-evaporation process by varying the 2nd stage growth temperature and their solar cell performances were evaluated. Although the higher growth temperature yielded (220) preferred orientation of CIGS, the solar cell performance was deteriorated mainly due to lower V_{oc} and FF. The flattened Ga profile and emerge of unknown phases, presumably Cu_{2-x}Se , are suggested to be responsible for the poor efficiency.

Acknowledgment

The authors appreciate the financial support from "Development of 25% Efficiency Grade Tandem CIGS Thin Film Solar Cell Core Technology" of MKE (Ministry of Knowledge Economy) and ISTK (Korea Research Council for Industrial Science and Technology) of Republic of Korea.

References

- [1] Ramanathan, K., Teeter, G., Keane, J. C., & Noufi, R., (2005). *Thin Solid Films*, 480–481, 499–502.
- [2] Jackson, Phill, Hariskos, Dimitrios, Lotter, Erwin, Paetel, Stefan, Wuerz, Roland, Menner, Richard, Wischmann, Wiltraud, & Powalla, Michael, (2011). *Progress in Photovoltaics : Research and Application*, 19, 894–897.
- [3] Lundberg, O., Edoff, M., & Stolt, L., (2004), *Thin solid Films*, 480–481. 520–525.
- [4] Repins, Ingrid, Contreras, Miguel A., Egaas, Brian, DeHart, Clay, Scharf, John, Perkins, Craig L., To, Boddy, & Noufi, Rommel, (2008). *Progress in Photovoltaics : Research and Application*, 16, 235–239.
- [5] Han, Sung-Ho, Hasoon, Falah S., Al-Thani, Hamda A., Hermann, Allen M., & Levi, Dean H., (2005). *Journal of Physics and Chemistry of Solids*, 66, 1895–1898.
- [6] Heath, J. T., Cohen, J. D., & Shafaman, W. N., (2003). *Thin Solid Films*, 431–432, 426–430.
- [7] Sato, T., Kawasaki, Y., Sugiyama, M., & Chichibu, S. F., (2011). *Japanese Journal of Applied Physics*, 50, 05FB05.
- [8] James, R. W., (1948). *The Optical Principles of the Diffraction of X-rays, Vol. II: The Crystalline State*, Bell & Sons, London, UK.
- [9] Chaisitsak, S., Yamada, A., & Konagai, M., (2002). *Jpn. J. Appl. Phys.* 41, 507–513.
- [10] Contreras, M. A., Egaas, B., Ramanathan, K., Hiltner, J., Swartzlander, A., Hasoon, F., & Noufi, R., (1999). *Prog. Photovolt.: Res. Appl.*, 7, 311.
- [11] Contreras, M. A., Jones, K. M., Gedvilas, L., and Matson, R., (2000). *16th European Photovoltaic Solar Energy Conference and Exhibition*, Glasgow, U.K, 732–735.
- [12] Dullweber, T., Hanna, G., Rau, U., & Schock, H. W., (2001). *Solar Energy Materials & Solar Cells*, 67, 145–150.
- [13] Nadenau, V., Hariskos, D., Schock, H.-W., Krejci, M., Haug, F.-J., Tiwari, A. N., Zogg, H., & Kostorz, G., (1999). *Journal of Applied Physics*, 85, 534–542.
- [14] Nadenau, V., Rau, U., Jasenek, A., & Schock, H.-W., (2000). *Journal of Applied Physics*, 87, 584–593.